NANO LETTERS

Letter

pubs.acs.org/NanoLett

Giant Suppression of Photobleaching for Single Molecule Detection via the Purcell Effect

Hu Cang,[†,‡] Yongmin Liu,[†,§,∥] Yuan Wang,[†] Xiaobo Yin,[†,⊥] and Xiang Zhang*[,†,⊥]

[†]NSF Nanoscale Science and Engineering Center (NSEC), 3112 Etcheverry Hall, University of California, Berkeley, California 94720, United States

[‡]Waitt Advanced Biophotonics Center, Salk Institute for Biological Studies, 10010 North Torrey Pines Road, San Diego, California 92037, United States

[§]Department of Mechanical and Industrial Engineering, Northeastern University, 360 Huntington Avenue, Boston, Massachusetts 02115, United States

[∥]Department of Electrical and Computer Engineering, Northeastern University, 360 Huntington Avenue, Boston, Massachusetts 02115, United States

[⊥]Materials Sciences Division, Lawrence Berkeley National Laboratory, 1 Cyclotron Road, Berkeley, California 94720, United States

Supporting Information

ABSTRACT: We report giant suppression of photobleaching and a prolonged lifespan of single fluorescent molecules via the Purcell effect in plasmonic nanostructures. The plasmonic structures enhance the spontaneous emission of excited fluorescent molecules, reduce the probability of activating photochemical reactions that destroy the molecules, and hence suppress the bleaching. Experimentally, we observe up to a 1000-fold increase in the total number of photons that we can harvest from a single fluorescent molecule before it bleaches. This approach demonstrates the potential of using the Purcell effect to manipulate photochemical reactions at the subwavelength scale.

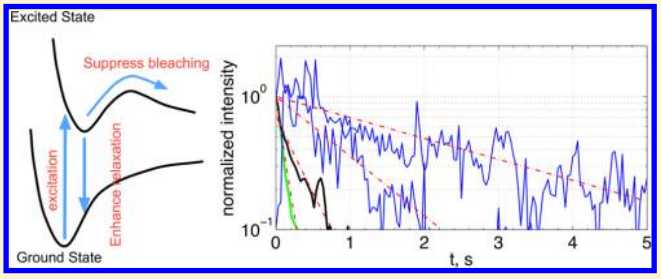

KEYWORDS: *Nano-optics, single-molecule fluorescence spectroscopy, plasmonics*

Photobleaching is a photochemical reaction of fluorescent molecules that irreversibly destroys their fluorescence capability. It determines the lifespan of a single fluorescent molecule and imposes a fundamental limit on the total number of photons that can be harvested from the molecule.[1,2] Considerable efforts have been devoted to suppressing photobleaching, which culminates primarily in chemical-based strategies that aim to make the local environment more chemically inert to fluorophores,[3,4] or modifying the structures and energy landscapes of fluorophores to be more resistant to photobleaching.[5,6] Progress has been achieved along these routes, including the discovery of oxygen scavenger systems,[3] photostable green fluorescent proteins,[5] and semiconductor quantum dots.[7] However, the increasing demand for more photons from a single molecule[1,8] requires new strategies beyond these chemical approaches.

Recent progress in plasmonics manifests a "physical" approach to address the challenge. Plasmonics[9−11] offer a new way to mediate the interaction between a molecule and its local electromagnetic environment.[12,13] The surface plasmon of metallic nanostructures allows for deep subwavelength confinement of light[14,15] and enhancement of the local density of optical states.[16,17] These structures can substantially enhance the spontaneous emission of fluorophores near the metal surface, that is, the so-called Purcell enhancement.[18−20] In contrast to photonic crystals,[21−24] the plasmonic Purcell enhancement is broadband. The impacts of the plasmonic Purcell enhancement on photostability have been noticed previously. For instance, Hale et al. have observed reduction of photo-oxidation of semiconducting polymer when doped with silica core-gold nanoshells,[25] and Muthu et al. and Malicka et al. have observed decreasing photobleaching of fluoresce dyes on the surface of thin silver films[26] and silver nanoparticles.[27] Recently, the Purcell effect has been further expanded to tune the spectroscopic properties of dye molecules to selectively remove a long-lived triplet state,[28] enhance the fluorescence signal,[29] suppress quantum dot blinking,[30] and manipulate selection rules.[31] A novel core−shell type of plasmonic nanocomposite structures has also been developed as nanocontainers to protect fluorescence dyes.[32] In particular, plasmonic nanoantennas,[17,22−24,33−35] a class of plasmonic structures, can couple light in and out with high efficiency and confine light field far below the diffraction limit and consequently boost the local density of optical states, providing

Received: August 14, 2013
Revised: November 9, 2013
Published: November 18, 2013

an ideal interface to enhance the interactions between photons and emitters that are normally weak due to the significant size mismatch between the wavelength of light and emitters. Most of the plasmonic antennas share a similar design of radio wave antennas, yet at a smaller, nanometer length scale. These include monopole,[21] dipole,[36] bowtie,[33] diabolo,[37] and dimer[38,39] antennas. The strong Purcell effect of the plasmonic nanoantennas have been shown to redirect emission direction from a single emitter[24,35] and enhance spontaneous emission rate by 2 orders of magnitude.[23] Here, we use a single-molecule approach to examine the suppression of photobleaching by the Purcell effect via plasmonic nanostructures and demonstrate that the strong Purcell effect of a dimer antenna can effectively steer a fluorophore away from photobleaching and significantly prolong the fluorophore's lifespan. Up to 1000-fold more photons have been harvested from a single fluorescent molecule, which will be complementary to the available chemical schemes and enhance the efficiency of single molecule sensing.

Figure 1a uses a two-level model to illustrate this physical approach.[40,41] After absorbing one quanta of energy from a photon with a rate constant of k_A, a molecule is excited to an excited state e from ground state g. Its destiny is then determined through competition between two processes. The first process is relaxation, whereby the molecule dissipates energy to emit another photon (spontaneous emission, or fluorescence, with rate k_f) or to heat (intrinsic nonradiative process with rate k_{iNR}) and relaxes back to the ground state; the molecule is then ready to be excited again. The second process is photobleaching with a rate constant of Γ, whereby the molecule breaks its chemical bonds or changes its structure permanently, thus leading to the loss of its fluorescence capability. Because the two channels—relaxation and bleaching—compete with each other, it is possible to reduce the probability of the molecule entering the bleaching channel by enhancing the relaxation process using plasmonic structures.

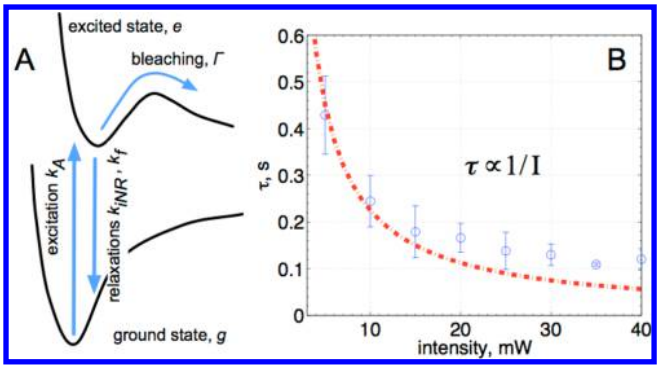

Figure 1. (a) After adsorbing a photon, the molecule reaches an excited state e from the ground state g. The excited molecule will most likely relax back to the ground state, but with a small probability, it suffers permanent damages as a result of a photochemical reaction—bleaching. (b) A control experiment measures the lifespan τ of chromeo-642 dyes on glass slide as a function of the excitation power I. An inverse relation (red dash–dot curve), $1/I$, can be seen in the figure. The discrepancy at higher excitation power is due to the limited time resolution of the experiments, which is 50 ms.

For a more quantitative description, we use a set of kinetics equations to model the excitation, the relaxation, and the bleaching process as follows:

$$\frac{\mathrm{d}}{\mathrm{d}t}e = -(k_f + k_{iNR} + \Gamma) + k_A g$$

$$\frac{\mathrm{d}}{\mathrm{d}t}g = (k_f + k_{iNR})e - k_A g \quad (1)$$

where e and g are probabilities of the molecule being at the excited and ground state, respectively, and k_A is the excitation rate for absorption of photons. Here we assume that the bleaching rate Γ is a constant,[42] and independent of the excitation laser intensity, because in our experiment a low-power continuous laser (5–40 mW) is used to illuminate a wide field ($100 \times 100\ \mu m^2$).

From eq 1 we can calculate the average lifespan of a fluorophore, that is, the time that a fluorophore continuously emits photons before it bleaches:

$$\tau = \int_0^\infty te(t)\,\mathrm{d}t \Big/ \int_0^\infty e(t)\,\mathrm{d}t = (k_f + k_{iNR} + k_A + \Gamma)/\Gamma k_A \quad (2)$$

We use the term "lifespan" to distinguish it from another term, "lifetime," which refers to the time it takes for an excited fluorophore to relax back to its ground state, defined as $1/(k_{iNR} + k_f)$. For most fluorophores, the relaxation rate k_{iNR} and k_f are in the order of 1 ns^{-1}, which is much larger than the bleaching rate constant Γ and the excitation rate constant k_A, both of which are around 1 ms^{-1}. Therefore, the average lifespan is:

$$\tau \approx k_f/\Gamma q k_A \quad (3)$$

where q is the fluorescence quantum yield of the fluorophore, defined as $q = k_f/(k_f + k_{iNR})$.

We also introduce the photobleaching limit—the total number of photons that a molecule has emitted before it photobleaches—as a metric:

$$P = \int \mathrm{d}t k_f e(t) = k_f/\Gamma \quad (4)$$

Compared with the lifespan, τ, the photobleaching limit, P, is a more suitable measure to evaluate the efficiency of photobleaching suppression. The reason for this is: First, the total number of photons is the most important parameter in many cases, such as in single-molecule fluorescence microscopy. Second, the lifespan, τ, strongly depends on the excitation intensity, I. One can see from eq 3 that τ is inversely proportional to the excitation rate, k_A, which is proportional to the excitation intensity, I. Therefore, although further exciting a fluorophore by increasing the excitation powers can make the fluorophore brighter, it also reduces the lifespan of the fluorophore. In contrast, the photobleaching limit of a molecule is a product of the lifespan and fluorescence intensity, which remains a constant over its entire lifespan, as determined by eq 4. The above kinetics equations provide a simplified model to understand the connection between bleaching and the Purcell effect, the two seemingly unrelated phenomena.

To confirm that the photobleaching limit is an excitation-independent metric, we performed a control experiment, as is shown in Figure 1b. A prism-type total-internal-reflection microscope (TIRF) is used in the experiments. The excitation source is a 644 nm (Coherent Inc. Cube 40 mW) laser. The saturation of adsorption typically occurs when there are more than one photon interacts with a molecule within the lifetime of the molecule, which is in the nanosecond range. In the experiment we used a lower-power CW laser (5–40 mW) and

dx.doi.org/10.1021/nl403047m | Nano Lett. 2013, 13, 5949–5953

a wide field TIRF excitation (100 × 100 μm^2), rather than a focused excitation; therefore, the photon density is much lower than necessary to reach the saturation. After flowing a solution of 1 nM chromeo642 dyes (Active Motif) into a quartz chamber, the dyes adsorb into the quartz surface. Immediately after the laser is turned on, the dyes start to bleach, and the total fluorescence intensity in the field of view decreases. Fitting the decay curves to a single exponential function yields the lifespan, τ. The lifespan is then plotted against the intensity of the excitation laser, I, where $1/I$ dependence of the lifespan is evident. Therefore, the total number of photons, which equals the product of the lifespan and the fluorescence intensity of the fluorophore, remains a constant of k_f/Γ. The time resolution of the experiments is 50 ms, limited by the frame rate of the camera. This contributes to the deviation of the measured results from the theoretical curve at higher excitation power in the figure.

Since the photobleaching limit, k_f/Γ, is determined by the competition between spontaneous emission, k_f, and photobleaching, Γ, both suppressing the bleaching rate, Γ, and enhancing the emission rate, k_f, via the Purcell effect can improve the photobleaching limit equally well. While chemical strategies have focused on reducing the bleaching rate, Γ, by modifying the molecular structures or chemical environment, this study demonstrates the giant suppression of photobleaching using a physical approach by enhancing spontaneous emission. Light−matter interaction can be substantially enhanced in engineered metallic nanostructures. As a result, high Purcell factors have been observed in a number of plasmonic systems that significantly increase spontaneous emission.[16,22,23] Denoting the increase of spontaneous emission as Purcell factor F_p, the spontaneous emission rate increases to $F_p k_f$. Spontaneous emission enhancement gives rise to both enhanced radiation and enhanced nonradiation (energy dissipation due to Ohmic losses). The enhancement of photostability of fluorphore by a plasmonic structure does not translate directly to the increase of total number of photons that can be harvested at far field, because the plasmonic structures introduce Ohmic loss as well, whereby energy transferred from the molecule is lost as heat. The amount of energy dissipation in the metal is deduced from numerical simulations, based on a semiclassical model (see Figure 4 and Supporting Information).[21,23] We introduce an efficiency factor η to model this effect, which characterize the portion of energy radiates to far field comparing to the total energy transferred from the molecule. Then the total number of photons that one can harvest from a single fluorophore becomes $F_p \eta k_f/\Gamma$. Therefore, we will observe $F_p \eta$-fold improvement beyond the photobleaching limit P (eq 4).

We used a self-assembly approach[43] to produce plasmonic nanostructures with finer features[17,22−24,33,34] that are critical to the high efficiency factor. A drop of gold nanoparticles (100 nm in diameter) in a water solution is deposited on the surface of a quartz slide. Upon drying, the nanoparticles aggregate and form a variety of clusters including di-, tri-, and multimers. Some of the clusters form structures with tight field confinement, a strong Purcell effect, and high efficiency factors that function as optical antennas. The distribution of the structures contributes to spreading the efficiency of the photobleaching suppression, which will be discussed later. Next, we mount the quartz slide on a total internal reflection (TIRF) microscope and flow in a chromeo-642 dye solution. The dye molecules adsorb onto the surface of the nanoparticles, and the fluorescence decays immediately after the excitation begins due to the photobleaching. When we compare the excited dyes at the same excitation power, but on a quartz surface, the bleaching is much slower (Figure 2b). The average lifespan of dyes from 24

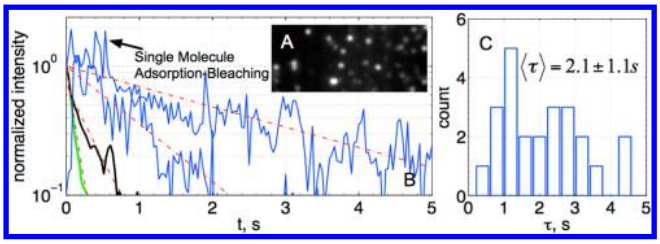

Figure 2. (a) One frame from a video measuring the lifespan of fluorescent molecules. The bright spots are fluorescence from the molecules on the nanoantennas. (b) The blue curves are decays of fluorescence from two bright spots due to the photobleaching. The red dash−dot lines are fit to a single exponential decay, yielding the decay constants of 0.97 ± 0.09 s and 2.76 ± 0.07 s, respectively. The power of the excitation laser is 10 mW. As a comparison, we plot the fluorescence decay of the same molecules on a quartz surface at a 10 mW (black) and 40 mW (green) excitation intensity respectively, in the same figure. The bleaching on the antennas is much slower. (c) A histogram of the fitted decay constants from 24 antennas, yields an averaged lifespan of 2.1 s, which is a 5-fold improvement comparing to the same molecules at the same excitation intensity (~0.4 s shown in Figure 1b).

nanostructures is 2.1 s (Figure 2c), which demonstrates an improvement of 5 times. However, because the local field in these nanostructures is much stronger than the excitation field due to the surface plasmon enhancement[14,23]—the lifespan of a dye is inversely proportional to the local field (Figure 1b)—the photobleaching suppression is actually much larger than 5 times.

To better measure the suppression of the photobleaching, we use a single molecule method to measure the total number of photons that a single fluorophore emits.[14] Briefly, the sample is submerged in a solution of chromeo-642 dyes, which randomly adsorb onto the surface of the nanostructures. Because the dye molecules diffuse much faster than the exposure time of a camera, the diffusing fluorophore yields a constant background. Once a single molecule adsorbs, a bright spot appears until the dye bleaches. The adsorbing−bleaching cycle appears as an intermittence pattern, which is a collection of single molecular events. The duration of each event corresponds to the lifespan of each molecule. Figure 3a and b present two typical single molecule events. In Figure 3a, one molecule continuously emits photons over 20 s, while the average lifespan of the same fluorophore is 0.4 s on the surface of a quartz substrate under the same excitation intensity of 5 mW (Figure 1b).

Figure 3c presents the giant suppression of photobleaching, which records each event as a data point on a log−log plot that correlates the lifespan of a molecule with its fluorescence intensity. The product of intensity (y-coordinate) and lifespan (x-coordinate) yields the total number of photons that a fluorophore has emitted during its lifespan. For the purpose of comparison, we conducted a control experiment on a bare quartz surface, and presented the data as black dots. A black dash line with slope −1 is drawn as a reference for the photobleaching limit. To help visualize the orders of magnitude of the suppression of photobleaching, we plot the multiple over the photobleaching limit as a series of black dashed lines marked with 1, 10, 100, and 1000.

dx.doi.org/10.1021/nl403047m | Nano Lett. 2013, 13, 5949−5953

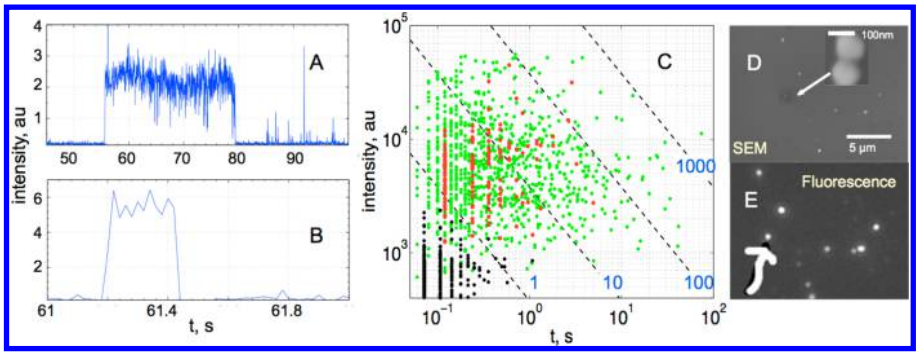

Figure 3. (a) The fluorescence intensity trace of a single molecule adsorption−bleaching event. The rising edge corresponds to the time the molecule adsorbs. The molecule photo bleaches after well over 20 s. Another molecule exhibiting stronger fluorescence but has shorter lifespan is shown in b. Each single molecule event is then plotted as a green dot in c, with the lifespan and the average fluorescence intensity corresponding to the *x*- and *y*-coordinates respectively. The power of the excitation laser is 5 mW. The black dots in c correspond to the result from a control experiment. A series of black dashed lines are plotted as eye-guides, corresponding to 1-, 10-, 100-, and 1000-fold improvement relative to the photobleaching limit. Most black dots, which are from the control experiment, are located below the line marked by 1. In contrast, the green dots, which are from plasmonic structures, are located above the line 1, with one of them even crossing the 1000-fold line. The red dots are the data taken from a dimer structure, whose SEM image and fluorescence images are shown in d−e. The inset of d is a zoomed-in view.

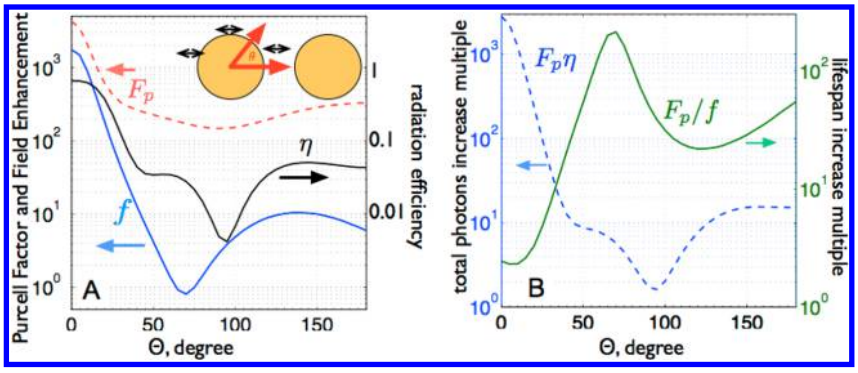

Figure 4. (a) A finite element simulation for a plasmonic structure consisting of two 100 nm gold spheres with a gap of 5 nm (schematically shown in the inset). The local excitation field enhancement factor $f = |E_{LOC}|^2/|E_0|^2$ (blue curve), the Purcell factor F_p (red dashed curve), and the radiation efficiency η (black curve), of a molecule is plotted against the location of the molecule adsorbed 2.5 nm above the surface of one sphere, represented by the polar angle θ. The increase of the lifespan F_p/f (green curve) and the increase of the total number of photons $F_p\eta$ (blue curve) are plotted in b. A molecule located at the center of the gap, corresponding to $\theta = 0$, exhibits a 3 orders of magnitude increase of the total photons.

The red dots in Figure 3c are all the events collected from one dimer structure and the colocalization images of scanning electron microscopy and fluorescence microscopy, as shown in Figure 3d and e. The red dots located primarily to the right of and above the photobleaching limit line indicate that these molecules have emitted more photons than the photobleaching limit. The green dots in Figure 3c represent single molecule events observed on the surface of various nanoparticle structures, which may include dimer, trimer, or multimers as a result of self-assembly. Most of the data points show 10- to 100-fold improvement, and the highest bleaching suppression factor reaches more than 1000-fold improvement. Some dye molecules may diffuse from the surface of gold nanoparticles before it photobleaches, leading to underestimation of the enhancement of the photo output. To further confirm our result, we conducted an experiment with thiol-tagged fluorescence oligo (Supporting Information). The thiol group has a strong affinity to the gold surface. We have observed very similar enhancement of the photon output (Figure S6).

The random adsorption of each molecule is a main factor that contributes to the broad distribution of the improvement, which corresponds to the spreading of the events plotted in Figure 3c, because each molecule experiences a different local density of state. We examine this factor qualitatively with a numerical simulation of a dimer structure[23] consisting of two 100-nm gold spheres separated by 5 nm. When a fluorophore adsorbs at the center of the gap, its radiation pattern matches the plasmonic mode of the structure, and the fluorophore experiences the strongest Purcell effect of $F_p \approx 4200$ (red dashed line, Figure 4a), the highest radiation efficiency of $\eta \approx 0.66$ (black line, Figure 4a), and the largest local field enhancement factor, $f = |E_{LOC}|^2/|E_0|^2 \approx 1800$ (blue line, Figure 4a). Furthermore, photobleaching reaches its highest suppression at $F_p\eta \approx 2700$ (blue dashed line, Figure 4b). When a molecule adsorbs at sites away from the center of the dimer, the structure operates less efficiently, and we see a quick decrease in the Purcell factor, F_p, the local field enhancement factor, f, and the efficiency of photobleaching suppression, $F_p\eta$. However, the lifespan of a fluorophore adjacent to the plasmonic structure exhibits a more complex behavior. An enhanced local field makes the fluorophore bleach faster, and a large Purcell factor, F_p, makes the fluorophore bleach slower. Because the field enhancement, f, is the strongest at the center of the dimer, the corresponding lifespan of the dye increases by a factor of F_p/f (approximately 1.28 times), while the total number of photons increases by 2700 times. Other factors, such as the size of the gap and the orientation of a fluorophore, are also critical. Discussions on these factors can be found in the

dx.doi.org/10.1021/nl403047m | *Nano Lett.* 2013, 13, 5949−5953

Supporting Information. Overall, the results from the numerical simulation of the enhancement of the photobleaching limit and lifespan are in agreement with the experiment (Figure 3). It is important to note that this is a general approach that results in significant improvement that complement the conventional chemical approaches. Additional single-molecule experiments with a different dye, chromeo-546, and a fluorescent protein, mCherry, yield similar results (Supporting Information).

In conclusion, we have demonstrated the suppression of photobleaching by up to 3 orders of magnitude through a physical approach based on the strong Purcell effect of plasmonic nanostructures. This dramatic enhancement, which has been difficult to achieve using chemical techniques alone, will significantly extend the lifespan of fluorophore and improve single-molecule imaging for biology. Furthermore, it suggests that nanophotonic structure can steer chemical reactions toward a desired direction.

■ ASSOCIATED CONTENT

Supporting Information

Kinetics equations for the photobleaching, Chromeo546 and RFP-mCherry, finite element simulation, and thiol-tagged DNA. This material is available free of charge via the Internet at http://pubs.acs.org.

■ AUTHOR INFORMATION

Corresponding Author

*E-mail: xiang@berkeley.edu.

Notes

The authors declare no competing financial interest.

■ ACKNOWLEDGMENTS

This research was supported by a Multidisciplinary University Research Initiative from the Air Force Office of Scientific Research (AFOSR MURI Award No. FA9550-12-1-0488) and Gordon and Betty Moore Foundation.

■ REFERENCES

(1) Moerner, W. E.; Fromm, D. P. *Rev. Sci. Instrum.* **2003**, *74*, 3597−3619.
(2) Hirschfeld, T. *Appl. Opt.* **1976**, *15*, 3135−3139.
(3) Benesch, R. E.; Benesch, R. *Science* **1953**, *118*, 447−449.
(4) Rasnik, I.; McKinney, S. A.; Ha, T. *Nat. Methods* **2006**, *3*, 891−893.
(5) Heim, R.; Cubitt, A. B.; Tsien, R. Y. *Nature* **1995**, *373*, 663−664.
(6) Panchuk-Voloshina, N.; Haugland, R. P.; Bishop-Stewart, J.; Bhalgat, M. K.; Millard, P. J.; Mao, F.; Leung, W.-Y.; Haugland, R. P. *J. Histochem. Cytochem.* **1999**, *47*, 1179−1188.
(7) Rossetti, R.; Nakahara, S.; Brus, L. E. *J. Chem. Phys.* **1983**, *79*, 1086−1088.
(8) Orrit, M.; Bernard, J. *Phys. Rev. Lett.* **1990**, *65*, 2716.
(9) Novotny, L.; Hecht, B. *Principles of Nano-Optics*; Cambridge University Press: Cambridge, 2006; p 558.
(10) Halas, N. J. *Nano Lett.* **2010**, *10*, 3816−3822.
(11) Barnes, W. L.; Dereux, A.; Ebbesen, T. W. *Nature* **2003**, *424*, 824−830.
(12) Moskovits, M. *J. Chem. Phys.* **1978**, *69*, 4159−4161.
(13) Gersten, J. I.; Nitzan, A. *Surf. Sci.* **1985**, *158*, 165−189.
(14) Cang, H.; Labno, A.; Lu, C.; Yin, X.; Liu, M.; Gladden, C.; Liu, Y.; Zhang, X. *Nature* **2011**, *469*, 385−8.
(15) Stockman, M. I.; Faleev, S. V.; Bergman, D. J. *Phys. Rev. Lett.* **2001**, *87*, 167401.
(16) Barnes, W. L. *J. Mod. Opt.* **1998**, *45*, 661−699.
(17) Bharadwaj, P.; Deutsch, B.; Novotny, L. *Adv. Opt. Photonics* **2009**, *1*, 438−483.
(18) Purcell, E. M. *Phys. Rev.* **1946**, *69*, 681.
(19) Kleppner, D. *Phys. Rev. Lett.* **1981**, *47*, 233.
(20) Yablonovitch, E. *Phys. Rev. Lett.* **1987**, *58*, 2059.
(21) Anger, P.; Bharadwaj, P.; Novotny, L. *Phys. Rev. Lett.* **2006**, *96*, 113002.
(22) Novotny, L.; van Hulst, N. *Nat. Photonics* **2011**, *5*, 83−90.
(23) Kinkhabwala, A.; Yu, Z.; Fan, S.; Avlasevich, Y.; Mullen, K.; Moerner, W. E. *Nat. Photonics* **2009**, *3*, 654−657.
(24) Curto, A. G.; Volpe, G.; Taminiau, T. H.; Kreuzer, M. P.; Quidant, R.; van Hulst, N. F. *Science* **2010**, *329*, 930−933.
(25) Hale, G. D.; Jackson, J. B.; Shmakova, O. E.; Lee, T. R.; Halas, N. J. *Appl. Phys. Lett.* **2001**, *78*, 1502−1504.
(26) Muthu, P.; Gryczynski, I.; Gryczynski, Z.; Talent, J.; Akopova, I.; Jain, K.; Borejdo, J. *Anal. Biochem.* **2007**, *366*, 228−236.
(27) Malicka, J.; Gryczynski, I.; Fang, J. Y.; Kusba, J.; Lakowicz, J. R. *J. Fluoresc.* **2002**, *12*, 439−447.
(28) Kena-Cohen, S.; Wiener, A.; Sivan, Y.; Stavrinou, P. N.; Bradley, D. D. C.; Horsfield, A.; Maier, S. A. *ACS Nano* **2011**, *5*, 9958−9965.
(29) Yuan, H.; Khatua, S.; Zijlstra, P.; Yorulmaz, M.; Orrit, M. *Angew. Chem., Int. Ed.* **2013**, *52*, 1217−1221.
(30) Bharadwaj, P.; Novotny, L. *Nano Lett.* **2011**, *11*, 2137−2141.
(31) Jain, P. K.; Ghosh, D.; Baer, R.; Rabani, E.; Alivisatos, A. P. *Proc. Natl. Acad. Sci. U.S.A.* **2012**, *109*, 8016−8019.
(32) Zaiba, S.; Lerouge, F.; Gabudean, A. M.; Focsan, M.; Lerme, J.; Gallavardin, T.; Maury, O.; Andraud, C.; Parola, S.; Baldeck, P. L. *Nano Lett.* **2011**, *11*, 2043−2047.
(33) Schuck, P. J.; Fromm, D. P.; Sundaramurthy, A.; Kino, G. S.; Moerner, W. E. *Phys. Rev. Lett.* **2005**, *94*, 017402.
(34) Taminiau, T. H.; Stefani, F. D.; Segerink, F. B.; van Hulst, N. F. *Nat. Photonics* **2008**, *2*, 234−237.
(35) Curto, A. G.; Taminiau, T. H.; Volpe, G.; Kreuzer, M. P.; Quidant, R.; van Hulst, N. F. *Nat. Commun.* **2013**, *4*, 1750.
(36) Muhlschlegel, P.; Eisler, H. J.; Martin, O. J.; Hecht, B.; Pohl, D. W. *Science* **2005**, *308*, 1607−9.
(37) Kang, J. H.; Kim, K.; Ee, H. S.; Lee, Y. H.; Yoon, T. Y.; Seo, M. K.; Park, H. G. *Nat. Commun.* **2011**, *2*, 582.
(38) Muskens, O. L.; Giannini, V.; Sanchez-Gil, J. A.; Gomez Rivas, J. *Opt. Express* **2007**, *15*, 17736−46.
(39) Alu, A.; Engheta, N. *Phys. Rev. B* **2008**, *78*, 045102.
(40) Turro, N. J. *Modern Molecular Photochemistry*; University Science Books: Herndon, VA, 1991; p 628.
(41) Lakowicz, J. R. *Principles of Fluorescence Spectroscopy*, 3rd ed.; Springer: New York, 2006.
(42) Vasilev, K.; Stefani, F. D.; Jacobsen, V.; Knoll, W.; Kreiter, M. *J. Chem. Phys.* **2004**, *120*, 6701.
(43) Camden, J. P.; Dieringer, J. A.; Wang, Y.; Masiello, D. J.; Marks, L. D.; Schatz, G. C.; Van Duyne, R. P. *J. Am. Chem. Soc.* **2008**, *130*, 12616−12617.